\



Bandwidth-tunable silicon nitride microring resonators

Jiacheng Liu(刘嘉成), Chao Wu(吴超), Gongyu Xia(夏功榆), Qilin Zheng(郑骑林), Zhihong Zhu(朱志宏), and Ping Xu(徐平)

Citation: Chin. Phys. B, 2022, 31 (**1**): 014201. DOI: 10.1088/1674-1056/ac2e64
Journal homepage: http://cpb.iphy.ac.cn; http://iopscience.iop.org/cpb

What follows is a list of articles you may be interested in

Near 100% spectral-purity photons from reconfigurable micro-rings

Pingyu Zhu(朱枰谕), Yingwen Liu(刘英文), Chao Wu(吴超), Shichuan Xue(薛诗川), Xinyao Yu(于馨瑶), Qilin Zheng(郑骑林), Yang Wang(王洋), Xiaogang Qiang(强晓刚), Junjie Wu(吴俊杰), and Ping Xu(徐平)
Chin. Phys. B, 2020, 29 (**11**): 114201. DOI: 10.1088/1674-1056/abbb28

Low-power electro-optic phase modulator based on multilayer graphene/silicon nitride waveguide

Lanting Ji(姬兰婷), Wei Chen(陈威), Yang Gao(高阳), Yan Xu(许言), Chi Wu(吴锜), Xibin Wang(王希斌), Yunji Yi(衣云骥), Baohua Li(李宝华), Xiaoqiang Sun(孙小强), Daming Zhang(张大明)
Chin. Phys. B, 2020, 29 (**8**): 084207. DOI: 10.1088/1674-1056/ab943b

Optical enhanced interferometry with two-mode squeezed twin-Fock states and parity detection

Li-Li Hou(侯丽丽), Shuai Wang(王帅), Xue-Fen Xu(许雪芬)
Chin. Phys. B, 2020, 29 (**3**): 034203. DOI: 10.1088/1674-1056/ab6837

Highly sensitive digital optical sensor with large measurement range based on the dual-microring resonator with waveguide-coupled feedback

Xiang Xing-Ye, Wang Kui-Ru, Yuan Jin-Hui, Jin Bo-Yuan, Sang Xin-Zhu, Yu Chong-Xiu
Chin. Phys. B, 2014, 23 (**3**): 034206. DOI: 10.1088/1674-1056/23/3/034206

Modeling and analysis of silicon-on-insulator elliptical microring resonators for future high-density integrated photonic circuits

Xiong Kang, Xiao Xi, Hu Ying-Tao, Li Zhi-Yong, Chu Tao, Yu Yu-De, Yu Jin-Zhong
Chin. Phys. B, 2012, 21 (**7**): 074203. DOI: 10.1088/1674-1056/21/7/074203

Bandwidth-tunable silicon nitride microring resonators

Jiacheng Liu(刘嘉成), Chao Wu(吴超), Gongyu Xia(夏功榆), Qilin Zheng(郑骑林), Zhihong Zhu(朱志宏), and Ping Xu(徐平)†

Hunan Provincial Key Laboratory of Novel Nano-Optoelectronic Information Materials and Device, Institute for Quantum Information and State Key Laboratory of High Performance Computing, College of Advanced Interdisciplinary Studies & College of Computer, National University of Defense Technology, Changsha 410073, *China*

(Received 30 September 2021; revised manuscript received 9 October 2021; accepted manuscript online 11 October 2021)

We designed a reconfigurable dual-interferometer coupled silicon nitride microring resonator. By tuning the integrated heater on interferometer's arms, the "critical coupling" bandwidth of resonant mode is continuously adjustable whose quality factor varies from 7.9×10^4 to 1.9×10^5 with the extinction ratio keeping higher than 25 dB. Also a variety of coupling spanning from "under-coupling" to "over-coupling" were achieved, showing the ability to tune the quality factor from 6.0×10^3 to 2.3×10^5. Our design can provide an adjustable filtering method on silicon nitride photonic chip and contribute to optimize the nonlinear process for quantum photonics and all-optical signal processing.

Keywords: silicon nitride, microring resonators, Mach–Zehnder interferometer, ring filter, nonlinear optics

PACS: 42.65.–k, 42.65.Wi **DOI:** 10.1088/1674-1056/ac2e64

1. Introduction

The silicon nitride (Si_3N_4) photonic platform which has a wide bandgap enabling operation across wavelengths from the near-ultraviolet to the mid-infrared, has a variety of applications such as low-threshold frequency combs,[1–3] high-precision sensing,[4,5] and frequency conversion.[6] Microring resonators are the typical device in the silicon nitride photonics platform owing to their large field enhancement. The quality factors or the coupling conditions of the reported silicon nitride microrings are mostly fixed. However, different applications have different requirements for the working state of the microring resonator. For quantum photonic applications, microrings have been used to achieve quantum dot filtering[7] to overcome the broadening and indistinguishability of quantum emitters,[8,9] therefore the microring's bandwidth needs to be adjustable and work at "critical coupling" to guarantee high extinction ratio. For some nonlinear process, like pulsed pumped four wave mixing,[10] micoring resonator needs to work in "overcoupling" to optimize the conversion efficiency. Hence a reconfigurable microring resonator with tunable coupling conditions are highly desired. Tunable rings have been reported on the platform of the silicon-on-insulator, such as the strategy by adopting MEMs actuators[11] or thermally-controlled transverse temperature gradient coupler[12,13] for rings. However, the MEMS-actuated ring occupies a large footprint and is sensitive to environmental factors. For the temperature gradient coupler, a large resonance shift always accompanies with the quality-factor tuning.

In 1995, Barbarossa *et al.* first proposed to adopt an asymmetric Mach–Zehnder interferometer (AMZI) as the coupler for the ring resonator.[14] The interferometer coupler can modulate the extrinsic quality factor, then the total quality factor will be regulated. Different coupling conditions being over-coupling, critical coupling or under-coupling will be meet for different applications, such as ingenious optical sensor and tunable bandwidth filter.[15–18] Recent studies[19–23] have shown this design can improve the spectral purity and photon pair brightness as well as the efficiency of four-wave-mixing. But all these studies are performed on the silicon-on-insulator platform.

Herein, we demonstrate a dual-interferometer coupled ring based on the silicon nitride microring resonator. Silicon nitride has a more widely transmission window and the waveguide has much lower transmission loss, hence the applications of a tunable ring resonator differs from the silicon ring resonator. Here in this work, the dual-interferometers coupled ring is demonstrated to realize a variety of working conditions spanning from the "undercoupling" to "over-coupling" when the heater on one of the interferometers is applied with different voltages. When two interferometers are coordinated, a continuously tunable critical-coupling with bandwidth varying from 0.008 nm to 0.21 nm was achieved while the extinction ratio was kept higher than 25 dB. These results indicate that this design will have wide applications in optical filtering, nonlinear optics and quantum optics.

2. Theory

The dual-interferometer coupled resonators is shown in Fig. 1(a). Phase tuning of the interferometer is accomplished by the integrated heaters. We can use the transfer matrix method to deal with the dual-interferometer coupled resonators, and the transmissions in the through and drop side are

†Corresponding author. E-mail: pingxu520@nju.edu.cn

© 2022 Chinese Physical Society and IOP Publishing Ltd

as follows:

$$\frac{P_{\text{through}}}{P_{\text{in}}} = \frac{t_1^2 + \alpha^2 t_2^2 - 2\alpha t_1 t_2 \cos(\varphi)}{1 + \alpha^2 t_1^2 t_2^2 - 2\alpha t_1 t_2 \cos(\varphi)}, \tag{1}$$

$$\frac{P_{\text{drop}}}{P_{\text{in}}} = \frac{k_1^2 k_2^2 \alpha}{1 + \alpha^2 t_1^2 t_2^2 - 2\alpha t_1 t_2 \cos(\varphi)}, \tag{2}$$

where $\varphi = n_{\text{eff}}(2\pi/\lambda)L$ represents the phase change propagating round trip in the microring resonator, α is the round-trip loss coefficient, L is the total length of the microring resonator and n_{eff} is the effective refractive index. $k_{1,2}$ and $t_{1,2}$ denote the waveguide effective amplitude cross-coupling and transmission coefficients. Assuming that the four amplitude transmission coefficients and coupling coefficients between waveguides are same and are denoted by $t_0 k_0$, we can write the effective amplitude transmission coefficient from the waveguide to the ring as

$$t_{1,2} = -k_0^2 + t_0^2 \exp\left[-\mathrm{i}\left(n_{\text{eff}}\frac{2\pi}{\lambda}\Delta L + \theta_{1,2}\right)\right], \tag{3}$$

where ΔL represents the length difference between the two arms of the interferometer, and we set the length difference equal to the roundtrip length of ring, *i.e.*, $\theta_{1,2}$ denotes the phase tuning by integrated heater. $\Delta L = L$ ensures the transmission of resonant modes kept to be modulated by the interferometer coupler synchronously. Figure 1(b) shows transmission spectra of the dual-interferometer coupled microring for the through side and drop side and the effective coupling coefficient.

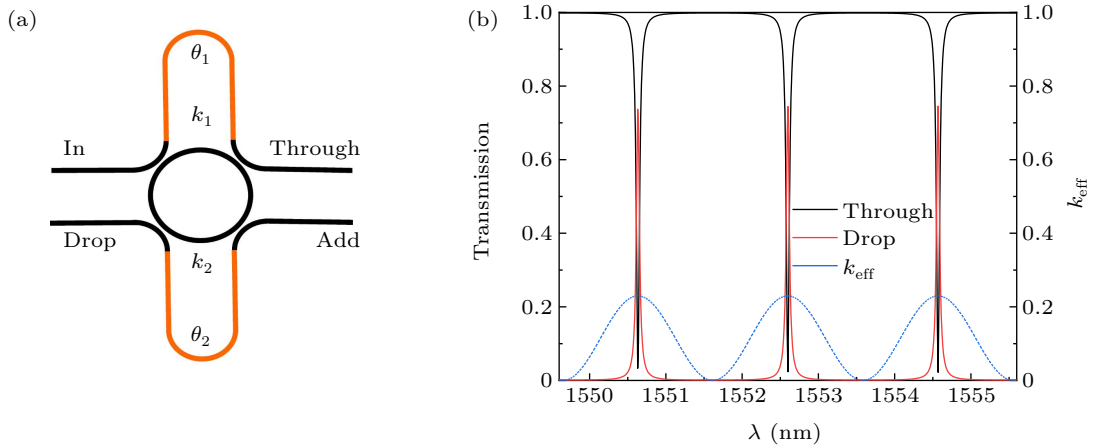


Fig. 1. (a) Schematic diagram of the dual-interferometer coupled microring. (b) The transmission spectra of the dual-interferometer coupled microring for the through side and drop side. The effective coupling coefficient is shown by the blue curve.

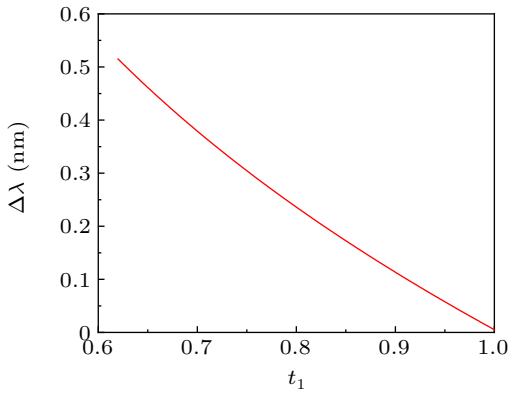


Fig. 2. The "critical coupling" bandwidths.

The full width at half-maximum bandwidth $\Delta\lambda$ can be written as

$$\Delta\lambda = \frac{(1 - at_1t_2)\lambda_{\text{r}}^2}{\pi n_{\text{g}} L\sqrt{t_1 t_2 a}}, \tag{4}$$

where λ_{r} and n_{g} are the resonant wavelength and group index. "critical coupling" condition of the dual-interferometer coupled resonator is $t_1(\theta_1) = at_2(\theta_2)$, and t_1 and t_2 are tunable which means that we can achieve "critical coupling" of different bandwidths. Here we set $\alpha = 0.995$ and $t_0 = 0.9$. After satisfying $t_1(\theta_1) = at_2(\theta_2)$, we calculate the "critical coupling" bandwidths in Fig. 2.

3. Experiment

The dual-interferometer coupled resonators are fabricated on the Si_3N_4 chip. The total length of resonator is 700 μm with the cross-section width and height at 800 nm and 1000 nm. The coupling distance between waveguides is 300 nm and the coupling length is 2 μm. The length difference between the two arms of the interferometer is 700 μm to ensure the same modulation to the resonant mode, and phase modulation is changed by the integrated heater above the waveguide. The fiber array is coupled to the side of the chip, with a total coupling loss of 8 dB. We measure the transmission spectrum by the transmitted power at different wavelengths. The linear propagation is measured to be 0.17 dB/cm.

Figure 3(a) shows the through port power transmission with both heaters off, and free spectral range is 1.68 nm. Figure 3(b) shows the quality factor with the voltage tuning of two heaters. The quality factor changes from 6.0×10^3 to 2.3×10^5 which indicates that the structure has a large tuning range. The

yellow line connects the points of "critical coupling", and this means that adjusting the two integrated heaters can find different $t_{1,2}$ to meet the $t_1(\theta_1) = at_2(\theta_2)$ conditions to achieve critical coupling.

In Fig. 4(a), t_1 is fixed and we tune the heater to change t_2. Under the tuning of the voltage, the microring resonator can achieve "over-coupling", "under-coupling", and "critical coupling" which confirms the capability of the device for tuning microring coupling states. In Fig. 4(b), we tune t_1 and t_2 respectively to achieve critical coupling of different bandwidths. The bandwidth changes from 0.21 nm to 0.008 nm, and the corresponding Q value changes from 7.9×10^4 to 1.9×10^5. At the same time, in the "critical coupling" state, the resonant mode can maintain extinction ratio of more than 25 dB.

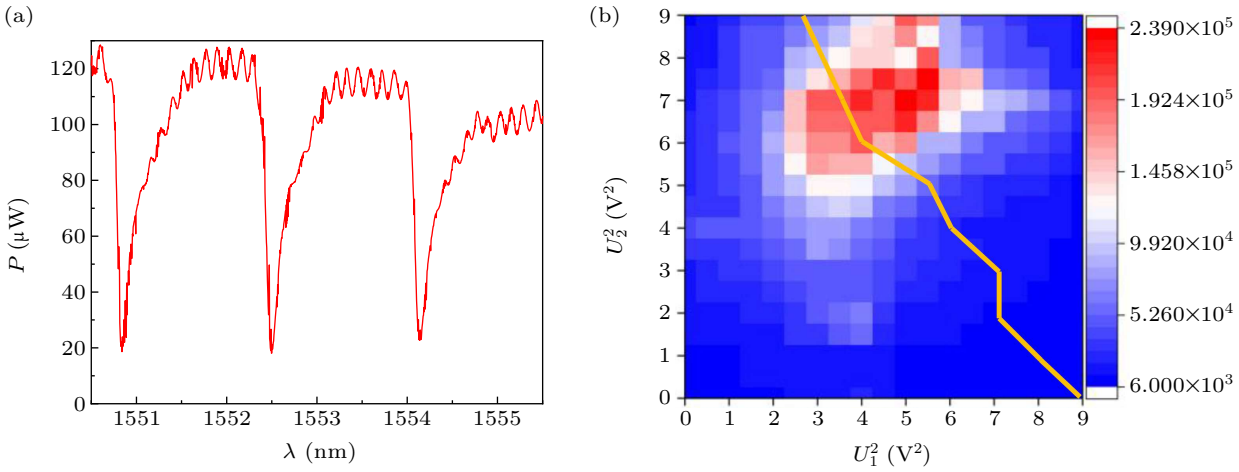


Fig. 3. (a) Measured through port power transmission with both heaters off. (b) The quality factor with the voltage tuning of two heaters. Yellow line connects the points of "critical coupling".

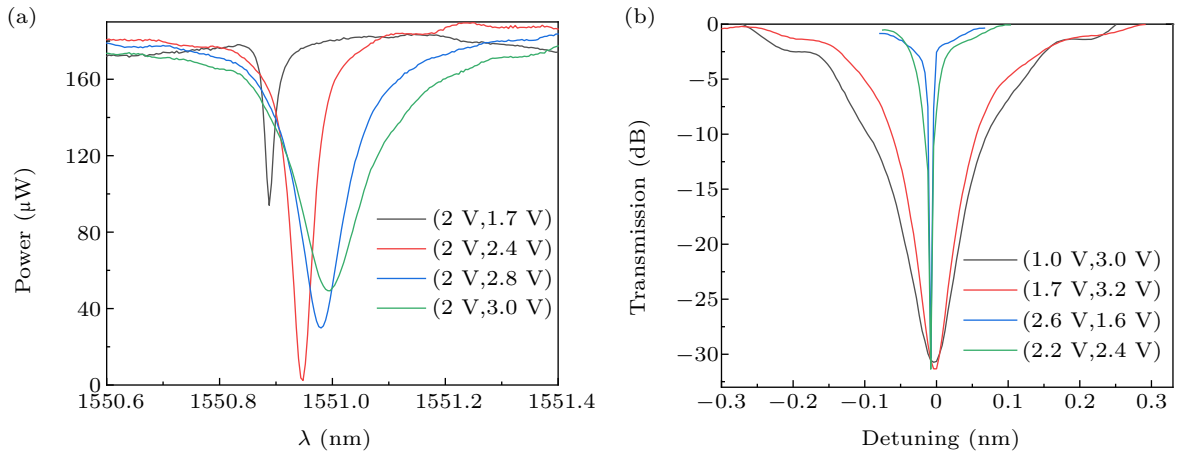


Fig. 4. (a) Transmission of "over-coupling", "under-coupling", and "critical coupling" with tuning of t_2 by heater voltage. (b) Transmission of different bandwidth "critical coupling" with tuning of t_1, t_2 by heater voltage.

4. Discussion and conclusion

We designed and fabricated reconfigurable dual-interferometer-coupled silicon nitride microring resonator. The continuous tunable, "overcoupling", "critical coupling", and "undercoupling" are realized and the bandwidth at critical coupling is also continuously adjustable. The reconfigurable dual-interferometer-coupled silicon nitride microring resonator will enable practical use in the research field of quantum photonic and all-optical signal processing.

Acknowledgments

Project supported by the National Key Research and Development Program of China (Grant Nos. 2019YFA0308700 and 2017YFA0303700), the National Natural Science Foundation of China (Grant Nos. 11627810 and 11690031), and the Open Funds from the State Key Laboratory of High Performance Computing of China (HPCL, National University of Defense Technology).

References

[1] Del'Haye P, Schliesser A, Arcizet O, Willen T, Holzwarth R and Kippenberg 2007 *Nature* **450** 1214
[2] Levy J S, Gondarenko A, Foster M A, Turner-Foster A C, Gaeta A L and Lipson M 2010 *Nat. Photon.* **4** 37
[3] Kippenberg T J, Holzwarth R and Diddams S A 2011 *Science* **332** 555
[4] Udem T, Holzwarth R and Hänsch T W 2002 *Nature* **416** 233
[5] Zhu J, Ozdemir S K, Xiao Y F, Li L, He L, Chen D R and Yang L 2010 *Nat. Photon.* **4** 46
[6] Li Q, Davanço M and Srinivasan K 2016 *Nat. Photon.* **10** 406

[7] Elshaari A W, Zadeh I E, Fognini A, Reimer M E, Dalacu D, Poole P J, Zwiller V and Jöns K D 2017 *Nat. Cummun.* **8** 379

[8] Reimer M E, Bulgarini G, Fognini A, Heeres R W, Witek B J, Versteegh A M, Rubino A, Braun T, Kamp M, Höfling S, Dalcacu D, Lapointe J, Poole P J and Zwiller V 2016 *Phys. Rev. B* **93** 195316

[9] Chen Y, Zadeh I E, Jöns K D, Fognini A, Reimer M E, Zhang J, Dalacu D, Poole P J, Ding F, Zwiller V and Schmidt O G 2016 *Appl. Phys. Lett.* **108** 182103

[10] Wu C, Liu Y, Gu X, Xue S, Yu X, Kong Y, Qiang X, Wu J, Zhu Z and Xu P 2019 *Chin. Phys. B* **28** 104211

[11] Lee M M and Wu M C 2006 *Opt. Express* **14** 4703

[12] Orlandi P, Morichetti F, Strain M J, Sorel M, Melloni A and Bassi P 2013 *Opt. Lett.* **38** 863

[13] Strain M J, Lacava C, Meriggi L, Cristiani I and Sorel M 2015 *Opt. Lett.* **40** 1274

[14] Barbarossa G, Matteo A M and Armenise M N 1995 *J. Light. Technol.* **13** 148

[15] Chen L, Sherwood-Droz N and Lipson M 2007 *Opt. Lett.* **32** 3361

[16] Shen H, Khan M H, Fan L, Zhan L, Xuan Y, Ouyang J, Varghese L T and Qi M 2010 *Opt. Express* **18** 18067

[17] Eid N, Boeck R, Jayatilleka H, Chrostowski L, Shi W and Jaeger N A F 2016 *Opt. Express* **24** 29009

[18] Wang J and Dai D 2010 *Opt. Express* **35** 4229

[19] Tison C C, Steidle J A, Fanto M L, Wang Z, Mogent N A, Rizzo A, Preble S F and Alsing P M 2017 *Opt. Express* **25** 33088

[20] Vernon Z, Menotti M, Tison C C, Steidle J A, Fanto M L, Thomas P, Preble S F, Smith A M, Asling P M and Liscidini M 2017 *Opt. Lett.* **42** 3638

[21] Heuck M, Pant M and Englund D 2018 *New J. Phys.* **20** 063046

[22] Liu Y, Wu C, Gu X, Kong Y, Yu X, Ge R, Cai X Z, Qiang X, Wu J, Yang X and Xu Ping 2020 *Opt. Lett.* **45** 73

[23] Wu C, Liu Y, Gu X, Yu X, Kong Y, Wang Y, Qiang X, Wu J, Zhu Z and Yang X 2020 *Sci. China-Physics Mech. & Astron.* **63** 220362